Prognostic Importance of Volumetric Measurements in Stage I Lung Adenocarcinoma[1]

Masahiro Yanagawa, MD, PhD
Yuko Tanaka, MD
Ann N. Leung, MD
Eiichi Morii, MD, PhD
Masahiko Kusumoto, MD, PhD
Shunichi Watanabe, MD, PhD
Hirokazu Watanabe, MD, PhD
Masayoshi Inoue, MD, PhD
Meinoshin Okumura, MD, PhD
Tomoko Gyobu, MD
Ken Ueda, MD
Osamu Honda, MD, PhD
Hiromitsu Sumikawa, MD, PhD
Takeshi Johkoh, MD, PhD
Noriyuki Tomiyama, MD, PhD

Purpose: To perform volumetric analysis of stage I lung adenocarcinomas by using an automated computer program and to determine value of volumetric computed tomographic (CT) measurements associated with prognostic factors and outcome.

Materials and Methods:- Consecutive patients (n = 145) with stage I lung adenocarcinoma who underwent surgery after preoperative chest CT were enrolled. By using volumetric automated computer-assisted analytic program, nodules were classified into three subgroups: pure ground glass, part solid, or solid. Total tumor volume, solid tumor volume, and percentage of solid volume of each cancer were calculated after eliminating vessel components. One radiologist measured the longest diameter of the solid tumor component and of total tumor with their ratio, which was defined as solid proportion. The value of these quantitative data by examining associations with pathologic prognostic factors and outcome measures (disease-free survival and overall survival) were analyzed with logistic regression and Cox proportional hazards regression models, respectively. Significant parameters identified at univariate analysis were included in the multiple analyses.

Results: All 22 recurrences occurred in patients with nodules classified as part solid or solid. Multiple logistic regression analysis revealed that percentage of solid volume of 63% or greater was an independent indicator associated with pleural invasion (P = .01). Multiple Cox proportional hazards regression analysis revealed that percentage of solid volume of 63% or greater was a significant indicator of lower disease-free survival (hazard ratio, 18.45 [95% confidence interval: 4.34, 78.49]; $P < .001$). Both solid tumor volume of 1.5 cm^3 or greater and percentage of solid volume of 63% or greater were significant indicators of decreased overall survival (hazard ratio, 5.92 and 9.60, respectively [95% confidence interval: 1.17, 30.33 and 1.17, 78.91, respectively]; P = .034 and .036, respectively).

Conclusion: Two volumetric measurements (solid volume, ≥1.5 cm^3; percentage of solid volume, ≥63%) were found to be independent indicators associated with increased likelihood of recurrence and/or death in patients with stage I adenocarcinoma.

[1] From the Department of Diagnostic Radiology, Stanford University School of Medicine, 1201 Welch Rd, Stanford, CA 94305 (M.Y., A.N.L.); Departments of Radiology (M.Y., T.G., K.U., O.H., H.S., N.T.), Pathology (E.M.), and Respiratory Surgery (S.W.), Osaka University Graduate School of Medicine, Suita, Osaka, Japan; Department of Radiology, Fujieda Municipal General Hospital, Fujieda, Shizuoka, Japan (E.M.); Department of Radiology (M.K., H.W.) and Division of Thoracic Surgery (M.I., M.O.), National Cancer Center, Tokyo, Japan; and Department of Radiology, Kinki Central Hospital of Mutual Aid Association of Public School Teachers, Itami, Hyogo, Japan (T.J.). Received August 13, 2013; revision requested September 16; revision received October 26; accepted December 10; final version accepted January 9, 2014. **Address correspondence to** M.Y. (e-mail: *m-yanagawa@radiol.med.osaka-u.ac.jp*).

Adenocarcinoma is the most common subtype of lung cancer. In 2011, a new classification of adenocarcinoma (1) was developed to standardize diagnostic criteria and terminology applied to the wide spectrum of entities encompassed in this histologic subtype, which can range from indolent to lethal tumors. Results from several studies (2–5) have shown by using computed tomographic (CT) imaging that morphologic structure of adenocarcinoma can be predictive of tumor grade and patient prognosis. As emphasized in the recently published recommendations for subsolid nodules from the Fleischner Society (6), measurement of solid components and determination of the relative percentages of solid versus ground-glass portions of subsolid nodules are important because an increase in the extent of a solid component is associated with a higher likelihood of an invasive tumor. However, integration of this type of prognostic CT data into clinical management algorithms for adenocarcinoma has been relatively hindered by the lack of standardized methods for tumor characterization and measurement, particularly in the setting of part-solid nodules.

Volumetric measurement of nodules is a promising technique that has been shown (7–11) to be both accurate and precise for the quantification of small solid nodules. However, volumetric assessment of subsolid nodules is more challenging because of difficulties in segmentation and accurate delineation between a tumor's ground-glass margins and the adjacent normal parenchyma. By using manual measurements, de Hoop et al (12) compared diameter, volume, and mass (volume × CT value) of 52 ground-glass nodules (GGNs) that were followed as part of a lung cancer screening trial; among the three measures, they found that mass of GGN was subject to less variability and allowed earliest detection of growth in malignant nodules. Ko et al (11) reported similar growth-related results in five solid and three subsolid malignant nodules that were detected earlier with volumetric measurements obtained by using a semiautomated computer algorithm than with radiologic criteria used in current practice.

We hypothesized that volumetric measurement of solid and nonsolid components of early-stage adenocarcinoma seen by using CT imaging can provide prognostic information. The purpose of our study was to perform volumetric analysis of stage I lung adenocarcinomas by using an automated computer program and to determine the value of volumetric CT measurements associated with prognostic factors and patient outcome.

Advances in Knowledge

- Automated volumetric analysis of stage I adenocarcinoma allowed quantification of CT features associated with patient outcome.
- Radiologist and software classification of nodules into subsolid and solid subtypes showed excellent agreement ($\kappa = 0.81$).
- Volumetric measurements of tumor solid component and percentage of solid volume were associated with recurrence and/or death, whereas measurement of total tumor volume was not.

Materials and Methods

Patients

We obtained approval from our internal institutional review board; informed consent was waived for retrospective review of patient records and images. The study population consisted of 145 consecutive patients (68 men and 77 women; mean age, 63.6 years ± 9.6 [standard deviation]; range, 31–82 years) who had undergone lobectomy ($n = 104$) or segmentectomy ($n = 41$) for pathologic stage I adenocarcinoma at our hospital from April 1999 to April 2006 and had a preoperative thin-section chest CT study available for review. All patients were node-negative based on fluorine 18 fluorodeoxyglucose (FDG) positron emission tomographic (PET) staging study. Hilar and mediastinal lymph node resections were performed in 104 patients with lobectomy, and hilar lymph nodal sampling was performed in 41 patients with segmentectomy at the time of tumor resection. Individuals who had history of adenocarcinoma of the lung or other organs or who had received induction chemotherapy before surgery were excluded from the study.

After hospital discharge, all patients were evaluated at 3-month intervals. The evaluation included a physical examination, chest x-ray, and blood tests (including tumor markers). Additional thoracoabdominal CT scans were generally obtained at 6-month intervals. Recurrence was confirmed at CT and, if necessary, FDG PET imaging. The median follow-up period of all 145 patients after surgery was 6.2 years (range, 0.86–12.63 years). Complete follow-up information until death or January 2013 was available for all patients. During the follow-up period, 22 patients experienced disease recurrence with seven associated cancer-related deaths.

Implication for Patient Care

- Automated volumetric analysis of early-stage adenocarcinomas can be associated with prognosis and may be helpful in determining appropriate treatment of patients with subsolid nodules.

Published online before print
10.1148/radiol.14131903 **Content codes:** CH OI

Radiology 2014; 272:557–567

Abbreviations:
FDG = fluorine 18 fluorodeoxyglucose
FWHM = full width at half maximum
GGN = ground-glass nodule

Author contributions:
Guarantors of integrity of entire study, M.Y., Y.T., S.W., H.W., T.G., K.U., O.H.; study concepts/study design or data acquisition or data analysis/interpretation, all authors; manuscript drafting or manuscript revision for important intellectual content, all authors; approval of final version of submitted manuscript, all authors; literature research, M.Y., Y.T., A.N.L., E.M., K.U., T.J.; clinical studies, M.Y., Y.T., E.M., M.K., S.W., H.W., M.I., M.O., O.H., H.S., T.J.; experimental studies, M.Y., Y.T., E.M., T.G., H.S., T.J.; statistical analysis, M.Y., A.N.L., E.M., M.K., S.W., H.W.; and manuscript editing, M.Y., A.N.L., E.M., O.H., T.J., N.T.

Conflicts of interest are listed at the end of this article.

Scanning Protocols

Chest CT scans were acquired by using a four-detector row CT scanner (LightSpeed QXi; GE Healthcare, Milwaukee, Wis) and an eight-detector row CT scanner (LightSpeed Ultra; GE Healthcare). Acquisition parameters were as follows: collimation, 0.625 mm or 1.25 mm; pitch, 0.625–1.5; rotation time, 0.4–0.8 seconds per rotation; exposure parameters, 120 kV and 200 mA; field of view, 200 mm. All image data were reconstructed with a high spatial frequency algorithm at contiguous section thicknesses of 0.625 mm or 1.25 mm.

Visual Analysis

CT scans were displayed on a monitor at lung window settings (level, −700 HU; width, 1200 HU). Two independent chest radiologists (G.T. and H.S., with 9 and 13 years of experience, respectively) visually classified tumors into three subgroups: pure GGN, part-solid GGN, and solid. GGN was defined as an area that exhibited a slight, homogeneous increase in density, which did not obscure underlying vascular markings. Solid was defined as an area of increased opacity that completely obscured underlying vascular markings. The two radiologists designated the distribution of each nodule as peripheral (outer one-third of lung, but not in contact with pleura), middle (inner two-thirds of lung), or juxtapleural (in contact with pleura). Final evaluations were decided by a consensus panel, which consisted of the same two radiologists and an adjudicator (O.H., with 21 years of experience in chest radiologic imaging), as needed. By using electronic calipers, one chest radiologist (M.Y., with 12 years of experience) measured the longest diameter of the solid component and of total tumor; solid proportion was defined as the ratio of the longest diameter of the solid component divided by the longest diameter of total tumor multiplied by 100%.

Computer Analysis

We developed our software by using commercial software (Microsoft Visual C++ 6.0; Microsoft, Redmond, Wash) on a commercially available personal computer. Incorporated in our software is a previously described (13) three-dimensional line filter that enabled the enhancement of curvilinear structures, such as vessels, in three-dimensional medical images on the basis of a combination of the eigenvalues of the three-dimensional Hessian matrix. Multiscale integration is formulated by taking the maximum among single scale filter responses, and its characteristics are examined to derive criteria for the selection of parameters in the formulation. The resultant multiscale line-filtered images provide improved segmentation and visualization of curvilinear structures. This three-dimensional line filter was used as the first step to eliminate vessels on the CT images (Fig 1). Quantitative analysis was then performed by one observer (M.Y., 12 years of experience in chest radiology) who was required to place an over-inclusive region of interest around each nodule after selecting a tumor center point (ie, a seed point) (Fig 2). The threshold value on CT between a tumor and surrounding normal lung parenchyma was automatically determined by applying CT density profile curves, one-dimensional quantitative CT values across the nodule, through the seed point at 10° intervals on each axial section (14) (Fig 3a). A CT value that corresponded to full width at half maximum (FWHM) was measured from each profile curve, and the mean FWHM from the 36 density profiles was used as threshold value (Fig 3b). FWHM is a mathematically well-defined parameter used to describe a measurement of the width of an object in imaging when that object does not have sharp edges. The width of the CT density profile curve is often decided by the FWHM (15,16). Following this approach, we used the CT value that corresponded to mean FWHM as an objective, standardized method to determine the threshold CT value between the tumor and surrounding normal lung parenchyma.

The tumor was also segmented by using a three-dimensional region-growing algorithm (17) that, after placement of an initial seed point, added in neighboring pixels with attenuation values above defined threshold value that did not contain vessels. The volume of the tumor was calculated as follows: (number of voxels within segmented region) × unit volume. Unit volume was defined as the product of x-, y-, and z-axes in a raw image.

On the basis of a previously reported threshold selection and nodule classification method (18), we used

Figure 1

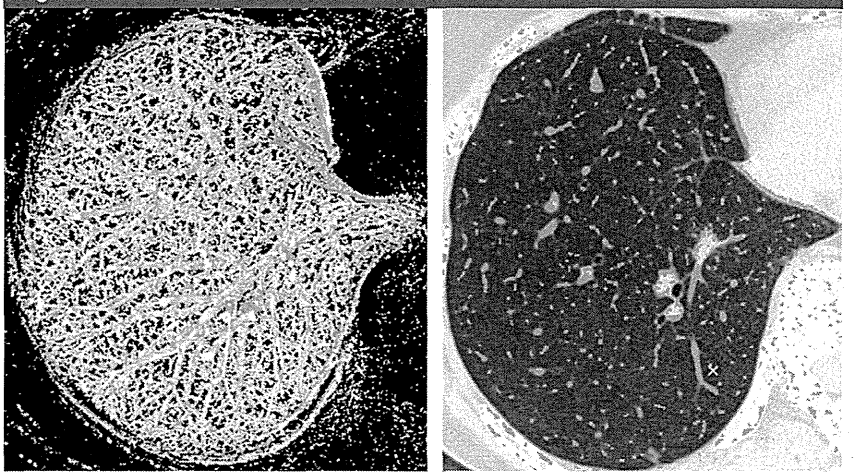

a. b.

Figure 1: Images show extraction of vessels by using a multiscale three-dimensional line filter. **(a)** Volume rendering image of all vessels identified by the three-dimensional line filter. **(b)** Green areas in right lung correspond to extracted vessels.

Figure 2

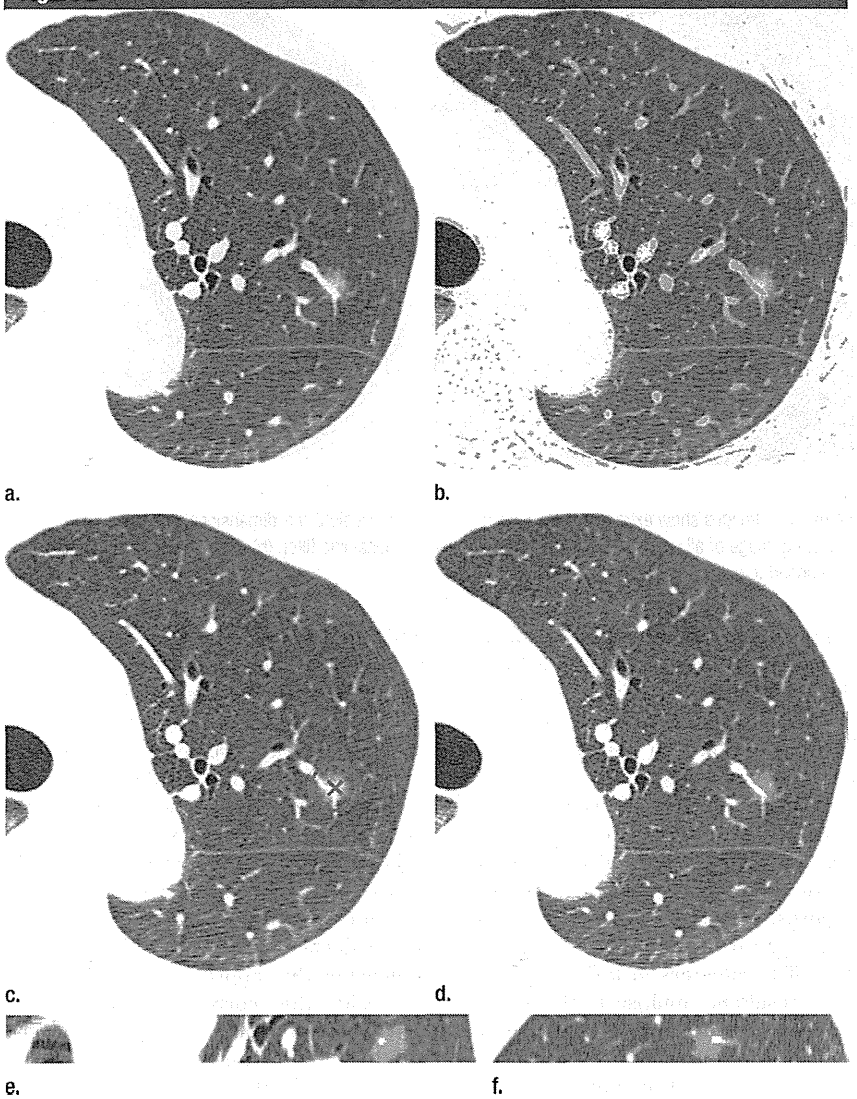

Figure 2: Images show sequential steps in volumetric analysis of a pure GGN in a 57-year-old woman. **(a)** Thin-section CT image shows a pulmonary vein traversing an 8.1-mm GGN in the left upper lobe. **(b)** Three-dimensional line filter identifies and extracts vessels (green areas). **(c)** An over-inclusive region of interest is drawn manually around the nodule in red. **(d)** Axial image, **(e)** coronal image, and **(f)** sagittal image of GGN. Nodule is automatically segmented (shown as highlighted green area) with calculation of GGN and solid components. Total volume, solid volume, and percentage of solid volume for this nodule are 0.14 cm^3, 0.00 cm^3, and 0.00%, respectively.

Figure 3

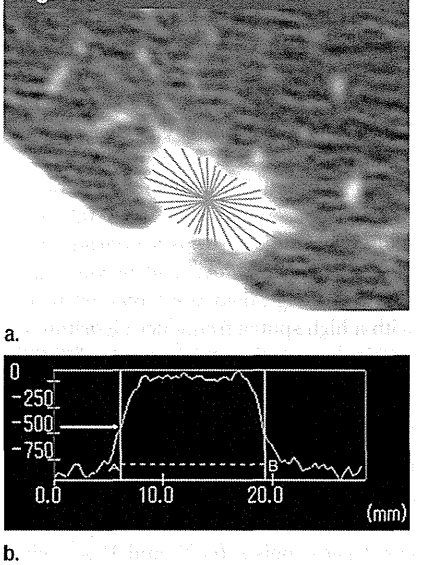

Figure 3: Threshold CT value between a tumor and surrounding normal lung parenchyma in a 60-year-old woman. **(a)** CT density profile curves are drawn through center of nodule at 10° intervals. **(b)** A representative profile curve shows CT value at FWHM is −545 HU (arrow). The mean CT value derived from all 36 profile curves on each axial section is used as the threshold CT value.

−291 HU as the threshold CT value between ground glass and solid. By using this value, each voxel of ground glass and solid included in a segmented tumor was automatically determined; total tumor volume, solid volume, and percentage of solid volume (solid volume/tumor volume × 100%) were calculated; and the nodule was classified into three subgroups (pure GGN [>98% of tumor with attenuation of −291 HU or less], part-solid GGN [2%–71.5% of tumor with attenuation greater than −291 HU], and solid [>71.5% of tumor with attenuation greater than −291 HU]) (18). Before beginning this study, we performed computer-assisted analysis of 10 nodules that were not included in this study that by qualitative evaluation consisted of pure ground-glass attenuation. In these 10 cases, percentage of solid volume ranged from 0% to 1.9% (mean, 0.8% ± 1.1% [standard deviation]); therefore, percentage of solid volume in the GGN subgroup was defined as less than 2%.

Pathologic Analysis

The presence of lymphatic, vascular, and pleural invasion was evaluated by two pathologists. Final evaluation was decided in consensus. Immunostaining methods by using D2-40 (Covance, San Diego, Calif), a lymphatic-specific monoclonal antibody, and CD31 (Dako, Glostrup, Denmark), an endothelial antigen, were performed to optimize identification of lymphatic and vascular channels, respectively (19,20).

Table 1

Quantitative Measurements in 145 Patients with Stage I Adenocarcinoma

Parameter	All Patients	Patients with Pure GGN	Patients with Part-Solid GGN	Patients with Solid Tumor
Visual analysis				
Longest diameter of tumor (mm)	15.7 ± 4.8 (7.0–31.0)	11.2 ± 2.7 (7.0–14.9)	15.9 ± 4.6 (7.2–31.0)	16.9 ± 5.1 (7.0–31.0)
Longest diameter of solid component (mm)	9.6 ± 7.0 (0.0–31.0)	0.0 ± 0.0 (0.0–0.0)	7.5 ± 4.7 (1.0–21.0)	16.9 ± 5.1 (7.0–31.0)
Solid proportion (%)	58.3 ± 37.1 (0.0–100.0)	0.0 ± 0.0 (0.0–0.0)	47.2 ± 26.5 (11.4–95.0)	100.0 ± 0.0 (100.0–100.0)
Computer analysis				
Tumor volume (cm^3)	2.46 ± 2.87 (0.03–16.97)	0.64 ± 0.54 (0.03–1.62)	1.92 ± 2.23 (0.05–15.60)	4.01 ± 3.58 (0.45–16.97)
Solid volume (cm^3)	1.47 ± 2.18 (0.00–14.28)	0.00 ± 0.02 (0.00–0.12)	0.75 ± 0.82 (0.003–4.09)	3.22 ± 3.00 (0.35–14.28)
Solid volume (%)	49.1 ± 28.2 (0.00–90.40)	0.21 ± 0.5 (0.00–1.90)	40.9 ± 19.9 (6.30–71.50)	78.7 ± 5.0 (71.60–90.40)

Note.—Data are mean ± standard deviation. Data in parentheses are range. For group classification, there were 145 patients total, 15 with pure GGN, 83 with part-solid GGN, and 47 with solid tumor. For visual analysis, there were 145 patients total, 15 with pure GGN, 86 with part-solid GGN, and 44 with solid tumor.

Statistical Analysis

We evaluated the value of eight features of CT (visual classification, software classification, longest diameter of solid component, longest diameter of total tumor, solid proportion, total tumor volume, solid volume, and percentage of solid volume) to examine associations with three prognostic factors (lymphatic invasion, vascular invasion, and pleural invasion) and two outcome measures (overall survival and disease-free survival). All statistical analyses were performed by using commercially available software (MedCalc version 8.0.0.1; Frank Schoonjans, Mariakerke, Belgium). Agreement between visual and software classification of nodule subgroups was evaluated by using the κ statistic, and it was classified as poor (κ = 0.00–0.20), fair (κ = 0.21–0.40), moderate (κ = 0.41–0.60), good (κ = 0.61–0.80), or excellent (κ = 0.81–1.00) (21). For each CT feature, the cutoff value that yielded the largest difference in numbers of patients with and without recurrence and death was determined by using the empirical receiver operating characteristic method. Receiver operating characteristic analyses were all univariate. The optimal thresholds were determined for each variable separately. Subsequently, associations between prognostic factors and each binary group designated by the cutoff value for the eight CT features were evaluated by using univariate logistic regression analysis. Similarly, associations between outcome measures and each binary group were evaluated by using univariate Cox proportional hazards regression analysis. Significant parameters identified by univariate analysis were included in the multiple logistic regression and Cox proportional hazards regression models (stepwise method; *P* value of .05 or less was used for entry into the model and *P* value greater than .1 was selected for removal), respectively. The 123 patients (85.0%) with no observed failure events in the present study were considered censored for the two outcome measures in the Cox proportional hazards regression model. Survival curves were generated by the Kaplan-Meier method, with comparisons performed by using the log-rank test. A *P* value of less than .05 indicated statistical significance.

Results

Visual and Computer Analyses

Results of all 145 patients are summarized in Table 1. Classification of nodules (per two radiologists) into pure GGN, part-solid GGN, and solid subtypes showed excellent agreement (κ = 0.90). There was excellent agreement (κ = 0.81) between visual and computer classification of nodule subgroups with disagreements on only five nodules.

Distribution of pure GGN was peripheral (*n* = 12), middle (*n* = 2), and juxtapleural (*n* = 1); distribution of part-solid GGN and solid nodules was peripheral (*n* = 72), middle (*n* = 8), and juxtapleural (*n* = 50). Mean measured longest diameter of solid component and total tumor were 9.6 mm ± 7.0 (range, 0–31.0 mm) and 15.7 mm ± 4.8 (range, 7.0–31.0 mm), respectively. Calculated solid proportion of nodules was 58.3%–37.1% (range, 0%–100%). Total tumor volume, solid volume, and percentage solid volume were 2.46 cm^3 ± 2.87 (range, 0.033–16.97 cm^3), 1.47 cm^3 ± 2.18 (range, 0–14.28 cm^3), and 49.1% ± 28.2 (range, 0%–90.4%), respectively.

Pathologic Analysis

There were identified lymphatic invasion in 17 cases, pleural invasion in 13 cases, and no cases of vascular invasion. There were 118 patients staged as pT1a, 14 patients staged as pT1b, and 13 patients staged as pT2. No patients were found to have lymph node metastases. According to pathologic analysis, there were 132 patients staged as Ia and 13 patients staged as Ib.

Relationship with Prognostic Factors

On the basis of receiver operating characteristic analysis, both visually and computer-classified subgroups were re-sorted into pure GGN and solid (part-solid GGN and solid) divisions. Cutoff values for the six CT features were as follows: longest diameter of solid component, 9.9 mm; longest tumor diameter, 18 mm; solid proportion, 78%; total tumor volume,

Table 2

Relationship of CT Features with Prognostic Factors

	Lymphatic Invasion (n = 145)			Pleural Invasion (n = 51)		
Logistic Regression Analysis	No. of Tumors	Odds Ratio	P Value	No. of Tumors	Odds Ratio	P Value
Univariate analysis						
Visual classification						
Pure GGN	15	1.96 (0.24, 15.97)	.49	1	ND*	ND*
Solid	130	…	…	50	ND*	ND*
Software classification						
Pure GGN	15	1.96 (0.24, 15.97)	.49	0	ND*	ND*
Solid	130	…	…	51	ND*	ND*
Longest diameter of tumor						
<18 mm	94	1.01 (0.35, 2.90)	.99	27	0.95 (0.27, 3.37)	.94
≥18 mm	51	…	…	24	…	…
Longest diameter of solid component						
<9.9 mm	81	2.17 (0.67, 6.99)	.19	21	3.00 (0.71, 12.65)	.13
≥9.9 mm	64	…	…	30	…	…
Solid proportion						
<78%	90	2.04 (0.65, 6.43)	.22	24	4.12 (0.98, 17.38)	.05
≥78%	55	…	…	27	…	…
Total tumor volume						
<1.9 cm^3	84	0.96 (0.34, 2.68)	.94	21	1.16 (0.32, 4.23)	.81
≥1.9 cm^3	61	…	…	30	…	…
Solid volume						
<1.5 cm^3	101	1.29 (0.45, 3.75)	.64	26	1.30 (0.37, 4.58)	.69
≥1.5 cm^3	44	…	…	25	…	…
Percentage of solid volume						
<63%	88	2.46 (0.88, 6.90)	.08	23	6.03 (1.58, 22.98)	.01
≥63%	57	…	…	28	…	…
Multiple analysis (by stepwise method)						
Percentage of solid volume						
<63%	88	ND	ND	23	6.03 (1.58, 22.98)	.01
≥63%	57	ND	ND	28	…	…

Note.—Data in parentheses are 95% confidence intervals. P values less than .05 indicated statistical significance. ND = no data.

* Statistical analysis for association with pleural invasion could not be performed because of a small number of juxtapleural nodules in GGN division.

1.9 cm^3; solid volume, 1.5 cm^3; and solid volume, 63%.

Results for association of eight CT features with two prognostic factors are summarized in Table 2. Statistical analysis was performed to examine associations with lymphatic invasion in 145 cases and pleural invasion in 51 cases; none of the resected tumors were found by using pathologic examination to have vascular invasion. Statistical analysis for examining the association with pleural invasion was performed only for those tumors that were juxtapleural in location. None of the eight CT features were found to be of use in examination of presence of lymphatic invasion. Univariate and multiple logistic regression analyses revealed that percentage of solid volume of 63% or greater was of significant use in examination of presence of pleural invasion (odds ratio, 6.03 [95% confidence interval: 1.58, 22.98]; P = .01).

Relationship with Recurrence and Survival

During a 7-year follow-up period, 22 patients experienced disease recurrence, and there were seven associated cancer-related deaths. All cases of recurrence and death occurred in patients with tumors classified as part-solid GGN (n = 6) or solid (n = 16); none occurred in patients with tumors classified as GGN.

Results for relationship of eight CT features with disease-free survival and overall survival are summarized in Table 3. Multiple analyses showed that percentage of solid volume of 63% or greater was a significant indicator for lower disease-free survival ($P < .001$). Both univariate and multiple analyses showed that solid volume of 1.5 cm^3 or greater and three-dimensional percentage of solid of 63% or greater were significant ($P < .05$) indicators for lower overall survival. Figures 4 and 5 show the lower disease-free and

Table 3

Association of CT Features with Survival

Cox Proportional Hazards Regression Analysis	No. of Tumors	Disease-free Survival		Overall Survival	
		Hazard Ratio	*P* Value	Hazard Ratio	*P* Value
Univariate analysis					
Visual classification					
Pure GGN	15	310644 (0.00, 3.48×10^{198})	.097	113504 (0.00, 5.23×10^{198})	.375
Solid	130	...	...	...	...
Software classification					
Pure GGN	15	310644 (0.00, 3.48×10^{198})	.097	113504 (0.00, 5.23×10^{198})	.375
Solid	130	...	...	...	...
Longest diameter of tumor					
<18 mm	94	2.89 (1.19, 6.98)	.012	2.65 (0.57, 12.22)	.207
≥18 mm	51	...	...	...	...
Longest diameter of solid component					
<9.9 mm	81	9.23 (2.74, 31.02)	<.001	7.93 (0.96, 65.19)	.055
≥9.9 mm	64	...	...	...	...
Solid proportion					
<78%	90	8.12 (2.76, 23.87)	<.001	4.32 (0.84, 22.08)	.080
≥78%	55	...	...	...	...
Total tumor volume					
<1.9 cm^3	84	4.57 (1.96, 11.43)	.001	3.81 (0.84, 12.31)	.086
≥1.9 cm^3	61	...	...	...	...
Solid volume					
<1.5 cm^3	101	7.17 (2.79, 18.35)	<.001	5.90 (1.17, 29.80)	.016
≥1.5 cm^3	44	...	...	...	...
Percentage of solid volume					
<63%	88	8.18 (2.80, 18.35)	<.001	9.58 (2.09, 43.91)	.01
≥63%	57	...	...	...	...
Multiple analysis (by stepwise method)					
Solid volume					
<1.5 cm^3	101	...	...	5.92 (1.17, 30.33)	.034
≥1.5 cm^3	44	...	...	...	...
Percentage of solid volume					
<63%	88	18.45 (4.34, 78.49)	<.001	9.60 (1.17, 78.91)	.036
≥63%	57	...	...	...	...

Note.—Data in parentheses are 95% confidence intervals. *P* values less than .05 indicate statistical significance.

overall survival for patients with solid volume of 1.5 cm^3 or greater (7-year disease-free survival and overall survival rates, 58.6% and 85.1%, respectively) and percentage of solid volume of 63% or greater (7-year disease-free survival and overall survival rates, 60.1% and 86.3%, respectively) compared with patients with solid volume less than 1.5 cm^3 (7-year disease-free survival and overall survival rates, 92.4% and 98.0%, respectively; $P \leq .015$) and percentage of solid volume of less than 63% (7-year disease-free survival and overall survival rates, 96.3% and 98.9%, respectively; $P \leq .01$).

Table 4 shows quantitative measurements, types of resection performed, and sites of recurrence in 22 patients with recurrence and death. Of the eight smallest tumors that were less than 15.5 mm in longest diameter, six tumors (75%) had solid volume of less than 1.5 cm^3 and one (13%) had percent solid volume of less than 63%. A 27-mm part-solid tumor that resulted in patient death had multiple foci of solid components with measured solid volume of 2.77 cm^3 and percentage of solid volume of 29.8% (Fig 6). Ten patients with recurrent disease presented with a solitary lung metastasis that (based upon either biopsy or resection findings) was confirmed to be adenocarcinoma. Only one nodule recurred in the primary tumor lobe of a patient who had undergone segmentectomy; the remaining nine nodules recurred in a nonprimary tumor lobe and were clinically judged to more likely represent metastatic disease than metachronous primaries based on temporal evolution as documented on postoperative surveillance imaging studies.

Figure 4

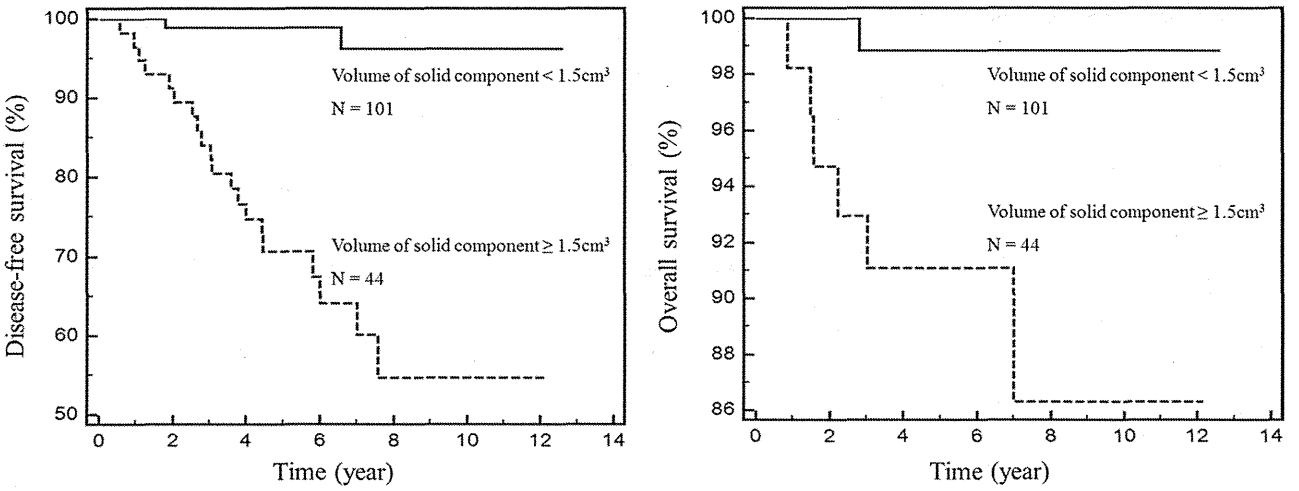

Figure 4: Kaplan-Meier survival curves show that patients with solid tumor volume of 1.5 cm^3 or greater had a significantly lower probability of **(a)** disease-free ($P < .001$) and **(b)** overall survival ($P = .015$) than patients with solid tumor volume less than 1.5 cm^3.

Figure 5

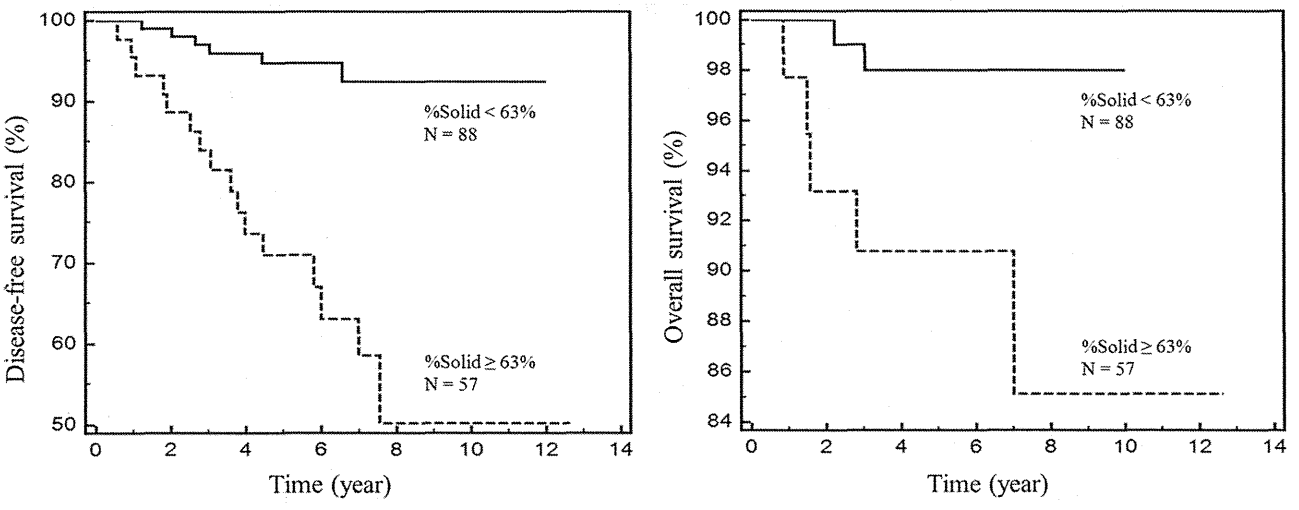

Figure 5: Kaplan-Meier survival curves show that patients with percentage of solid tumor volume of 63% or greater had a significantly lower probability of **(a)** disease-free ($P < .001$) and **(b)** overall survival ($P = .010$) than patients with percentage of solid tumor volume of less than 63%.

Discussion

Clinical algorithms for optimal management of adenocarcinomas that manifest as subsolid nodules by using CT imaging remain an area of active controversy. In two guidelines recently published by the Fleischner Society (6) and American College of Chest Physicians (22), there was disagreement as to whether total diameter or diameter of only the solid component of a part-solid GGN should be used as the predictive feature that determines triage into alternate management pathways. A more fundamental controversy is whether solid tumor components visualized by using CT imaging should be measured on mediastinal or lung windows (23).

In our study, we used a volumetric automated computer-assisted method to analyze early-stage adenocarcinomas and link the analytic output, including volumetric measurements, to prognostic

Table 4

Quantitative Measurements in 22 Patients with Recurrence and Death

Case No.	Longest Diameter of Tumor (mm)	Longest Diameter of Solid Component (mm)	Solid Proportion (%)	Total Volume (cm^3)	Solid Volume (cm^3)	Percentage of Solid Volume (%)	Type of Surgery	Site of Recurrence
Recurrence								
1	13.7	4.8	35.04	1.26	0.48*	38.1†	Seg (LLL)	Lung (RUL)
2	19	16.7	87.89	2.88	2.04	70.8	L (LUL)	Lung (LLL)
3	21.4	18.1	84.58	4.5	2.87	63.8	Seg (LUL)	Lung (LUL)
4	10	10	100	0.45	0.34*	75.6	Seg (RLL)	Lung (multiple)
5	12	12	100	0.82	0.67*	81.7	L (RML)	Lung (RUL)
6	12	12	100	0.9	0.62*	68.9	Seg (LUL)	Lung (RML)
7	13.3	13.3	100	2.38	1.92	80.7	L (RUL)	Lung (LLL)
8	16	16	100	2.04	1.82	89.2	L (RUL)	Lymph node
9	18.5	14.5	78.38	2.44	1.8	73.8	L (LUL)	Bone
10	21	21	100	5.14	3.99	77.6	L (RML)	Lymph node
11	21.5	21.5	100	4.75	4.04	85.1	L (RLL)	Lung (LLL)
12	29.2	29.2	100	12.38	10.55	85.2	L (LLL)	Lymph node
13	18	18	100	3.35	2.92	87.2	L (RLL)	Lung (multiple)
14	19.1	19.1	100	3.28	2.78	84.8	Seg (LLL)	Lung (LUL)
15	22.1	22.1	100	6.53	4.93	75.5	L (RUL)	Lymph node
Death								
16	27.1	15	55.35	9.31	2.77	29.8†	Seg (RUL)	Pleura
17	15.3	10	65.36	0.74	0.48*	64.9	L (LUL)	Brain
18	12	12	100	0.87	0.64*	73.6	Seg (RLL)	Lymph node
19	15.1	15.1	100	4.46	4.01	89.9	L (LUL)	Lung (RUL)
20	18.3	18.3	100	1.95	1.53	78.5	Seg (LUL)	Lung (LUL)
21	19.9	19.9	100	4.09	3.18	77.8	L (RML)	Pleura
22	22.2	22.2	100	6.33	4.69	74.1	L (LLL)	Pleura

Note.—Information in parentheses is excision cite. L = lobectomy, Seg = segmentectomy, RUL = right upper lobe, RML = right middle lobe, RLL = right lower lobe, LUL = left upper lobe, LLL = left lower lobe.

* Volume of solid component was less than 1.5 cm^3.

† Percentage of solid volume was less than 63%.

factors and outcome measures. By using our custom software, automatic classification of nodules had excellent agreement with visual classification by radiologists; pure GGNs classified visually and by using software were associated with excellent prognosis with no recurrences or death observed. The uniformly excellent prognosis of pure GGNs after resection has been reported by several groups (24–26), and we are unaware of any cases of recurrence, even when nodules less than 3 cm of pure ground-glass composition are eventually found at pathologic examination to have invasive components (26).

Accurate segmentation of pulmonary nodules with or without ground-glass component is a challenging problem (27–31). In general, nodule segmentation is performed by using a combination of watershed and shape-analysis techniques; however, because these methods are edge-based, they cannot accurately delineate GGNs that typically share blurred margins with the surrounding lung parenchyma. Tan et al (31) have developed a probability-based method for segmentation of ground-glass nodules by using a Markov random model. By using this technique, the average overlap between computer and manual results for six nodules that contain ground-glass components was 60%. Kim et al (32) demonstrated that volumetric analysis was applicable for volume and mass measurement (12) of both pure and part-solid GGNs without measurement variation. In our study, we elected to segment nodules by using the mean FWHM of multiple density profile curves found by using CT imaging, drawn through the center of each tumor, with recognition that this would be an imperfect but reproducible technique that likely underestimates the extent of peripheral ground glass in some cases of part-solid GGNs. Incorporation of a three-dimensional line filter in our software also allowed for the elimination of both contiguous and intralesional vessels that may artificially increase the calculated total tumor or solid tumor volume measurements, respectively.

Similar to previous studies (4,33–35), we found that for stage I adenocarcinoma, measurement of total tumor was associated less with prognostic factors and outcome than it was with measurements of the solid component. In our study, percentage of solid volume of 63% or greater was associated

Figure 6

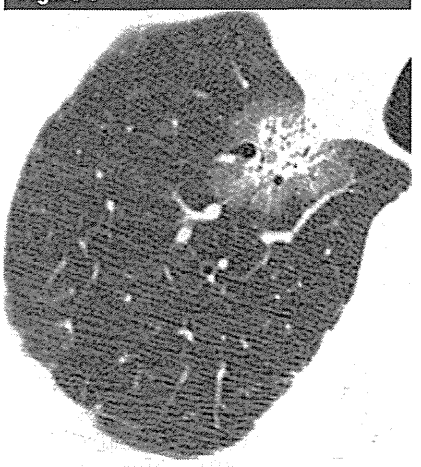

Figure 6: Thin-section CT image of a 27-mm nodule with multiple foci of solid components in a 65-year-old man who eventually died of recurrent disease. Volumetric measurements were total tumor volume, 9.31 cm^3; solid tumor volume, 2.77 cm^3; and percentage of solid tumor volume, 29.8%.

with the presence of pleural invasion; none of the four volumetric measurements were found to be associated with lymphatic or vascular invasion. This latter finding is discordant with results reported by Tsutani et al (33), who found that in 502 patients with clinical stage IA adenocarcinoma, solid tumor diameter was predictive of pleural, as well as of vascular and lymphatic invasion. Difference in results may be related to differences in the enrolled patient populations because our study included patients with pathologic stage I adenocarcinoma without lymph node metastases, and who therefore had a correspondingly lower prevalence of lymphatic invasion, vascular invasion, and pleural invasion compared with the population studied by Tsutani et al.

By using our volumetric automated computer-assisted analytic program, we found two volumetric measurements, solid volume of 1.5 cm^3 or greater and percentage of solid volume of 63% or greater, to be independent indicators associated with recurrence and/or death in patients with stage I adenocarcinoma. These results are consistent with those of previous studies that also reported that features found by using CT imaging, such as maximum diameter of the solid component (4,33) and ratio of maximum diameter of solid to ground-glass components exceeding 50% (2,36), can be associated with tumor recurrence after surgery. In our study, the two volumetric measurements were complementary, and used in combination they correctly identified 21 of 22 (95%) recurrent tumors. However, none of our evaluated two-dimensional measurements were found at multivariate analysis to be independent indicators associated with outcome; this lack of statistically significant results at multivariate analysis likely reflects the high degree of correlation between two-dimensional and volumetric variables and suggests that of the two quantitative sets, volumetric measurements may serve as better indicators associated with outcome. Compared with two-dimensional analysis that typically consists of tumor measurements on one or two images, volumetric analysis enables a more comprehensive and representative evaluation that may be particularly important for adenocarcinomas that have multiple foci of solid components.

Our study had several limitations. The study was retrospective in nature, and the relatively small number of enrolled patients may have resulted in inadequate statistical power to detect some CT features associated with prognosis. Results found in our study that had no statistically significant differences may have been caused by a true lack of differences or by the small sample size. Prospective studies with larger sample sizes will be needed to validate our results. Segmentation of subsolid nodules by using our custom software was imperfect with underestimation of the extent of peripheral ground glass. Given that ground glass is known to correspond to the lepidic noninvasive component of tumor, we chose not to perform manual edits so as to avoid the introduction of observer variability. Computer analysis of nodules was performed by only one operator who was required to select a tumor center point and draw an over-inclusive region of interest around the nodule before automated volumetric measurements could be performed. Ideally, the inclusion of one or more additional operators would have allowed for assessment of the reproducibility of the computer-generated volumetric measurements. Finally, inconsistency in the types of operations may have negatively affected outcomes in some patients who underwent sublobar resection; there are currently two ongoing randomized trials in Japan and North America to address whether segmentectomy can replace lobectomy as standard treatment (1).

In conclusion, our results demonstrated that two volumetric measurements (solid volume of ≥1.5 cm^3 and percentage of solid volume of ≥63%) are independent and complementary indicators associated with recurrence and/or death in patients with stage I adenocarcinoma. These results may have implications for determination of the optimal management of subsolid nodules.

Disclosures of Conflicts of Interest: M.Y. No relevant conflicts of interest to disclose. **Y.T.** No relevant conflicts of interest to disclose. **A.N.L.** No relevant conflicts of interest to disclose. **E.M.** No relevant conflicts of interest to disclose. **M.K.** No relevant conflicts of interest to disclose. **S.W.** No relevant conflicts of interest to disclose. **H.W.** No relevant conflicts of interest to disclose. **M.I.** No relevant conflicts of interest to disclose. **M.O.** No relevant conflicts of interest to disclose. **T.G.** No relevant conflicts of interest to disclose. **K.U.** No relevant conflicts of interest to disclose. **O.H.** No relevant conflicts of interest to disclose. **H.S.** No relevant conflicts of interest to disclose. **T.J.** No relevant conflicts of interest to disclose. **N.T.** No relevant conflicts of interest to disclose.

References

1. Travis WD, Brambilla E, Noguchi M, et al. International association for the study of lung cancer/american thoracic society/european respiratory society international multidisciplinary classification of lung adenocarcinoma. J Thorac Oncol 2011;6(2):244–285.

2. Ikehara M, Saito H, Yamada K, et al. Prognosis of small adenocarcinoma of the lung based on thin-section computed tomography and pathological preparations. J Comput Assist Tomogr 2008;32(3):426–431.

3. Nakazono T, Sakao Y, Yamaguchi K, Imai S, Kumazoe H, Kudo S. Subtypes of peripheral adenocarcinoma of the lung: dif-